Retardation effects in atomic bremsstrahlung

A. D. González, M. C. Pacher, and J. E. Miraglia
Instituto de Astronomía y Física del Espacio, Consejo Nacional de Investigaciones Científicas y Técnicas, Casilla de Correo 67, Sucursal 28, 1428 Buenos Aires, Argentina
(Received 21 October 1987)

Angular distributions of continuum radiation emitted during proton–aluminum-atom collisions are investigated. Atomic bremsstrahlung (AB) including retardation effects is calculated and compared with available experimental data. Angular distributions are found to be asymmetric with the maximum shifted towards angles smaller than 90°. A good agreement with the experiments is found where AB is dominant over the secondary-electron bremsstrahlung, i.e., for photon energies larger than $T_m = 2v^2$, where v is the ion velocity.

I. INTRODUCTION

In a previous paper,[1] we developed a general formulation (including retardation) to treat radiative emission of a colliding three-particle system in the nonrelativistic regime. Atomic bremsstrahlung (AB) and other radiative processes were studied in the dipole limit. In a subsequent paper[2] we applied that formulation to calculate radiative electron capture with retardation. Angular distributions were found to be in accordance with the experimental findings.

In the present work we calculate AB with retardation. This means that the photon momentum $\mathbf{k}$ is taken into consideration (in the dipole approximation $\mathbf{k}=\mathbf{0}$). AB and secondary-electron bremsstrahlung (SEB) have attracted considerable interest due to their important role in the PIXE (particle-induced x-ray-emission) technique. Both processes provide continuum backgrounds covering the characteristic lines of the trace-element analysis. The dipole approximation leads to $\sin^2\theta_\omega$-type photon distributions but the inclusion of retardation generally shifts it. The knowledge of that asymmetry is useful to improve PIXE measurements. Since SEB presents forward-shifted angular distributions, Ishii *et al.*[3] concluded that PIXE should be made at backward angles. Here we analyze higher photon energies where AB is supposed to be dominant over SEB. We anticipate that AB also presents forward-shifted angular distributions.

SEB is a two-step process: the target electrons are first ionized by the impinging projectile, and afterwards they undergo bremsstrahlung during close collisions with another target nucleus.[4] In the laboratory frame, those ionized electrons can acquire any final kinetic energy up to about $T_m = 0.5(2v)^2 = 2v^2$ (atomic units are used except where otherwise indicated). Therefore SEB x-ray production is expected to fall off sharply for $\omega > T_m$, as found in the experiments by Ishii, Morita, and coworkers.[5–7] In that region AB is supposed to dominate.

AB is a one-step process where the target electrons undergo bremsstrahlung in the presence of the passing projectile. Finally, the electrons end up in the same quantum state as the initial one, while the projectile indirectly transfers part of its kinetic energy to the radiation field. This mechanism has been introduced by Amusia[8] in the electron-atom context. Later on, AB was calculated with a second Born approximation by Ishii and Morita[9] [who previously called it radiative elastic scattering, RES (Ref. 10)] and we calculated it with the distorted-wave eikonal approximation and called it REL.[1] These names represent the same process calculated with different approaches to the scattering wave functions. To avoid proliferation of terminology, here we call it AB.

The work is organized as follows: In Sec. II we summarize the corresponding theory in Sec. III we compare our theoretical results with the experiments and draw conclusions.

II. THEORY

Let us assume a collision where a projectile (P) collides with an atom composed of a nucleus target (T) and an active electron (e). To first perturbative order, the radiation-matter matrix element can be separated into three terms representing the radiation of the center of mass, the internuclear and electron bremsstrahlung. In Ref. 1 we have calculated AB cross sections by using the symmetric eikonal wave functions in the dipole limit. In that case angular distributions were found to be symmetric, in agreement with the theoretical results of Ishii and Morita[9] (see Fig. 3 of Ref. 1). We have verified that the eikonal wave functions are off-shell orthogonal as are the exact ones, and so no spurious radiation is expected in the dipole limit.[11]

When retardation effects are included in radiative electron capture (REC), we found that the center-of-mass term does not vanish, and therefore it genuinely radiates.[2] In AB, the process studied here, the use of the eikonal wave functions eliminates the radiation of the center of mass and internuclear terms leaving only the electron bremsstrahlung (for $M_{T,P} \gg 1$).

When the photon momentum is not neglected, the electron-bremsstrahlung term reads (see Ref. 1 for details)

$$H_l^{\mathrm{EB}} = -iA_0\hat{\lambda}_l\cdot\exp\{-i\mathbf{k}\cdot[\mathbf{X}+(M_T/M_3)\mathbf{r}_T + (M_P/M_3)\mathbf{r}_P]\}\nabla_{\mathbf{r}_T}\ , \quad (2.1)$$

where $M_{T,P}$ are the projectile and target masses, $M_3 = M_T + M_P + 1$, $\hat{\lambda}_l$ is the polarization unit vector, $A_0 = (2\pi/\omega)^{1/2}$, where ω is the photon energy. $\mathbf{X}$ is the position of the center of mass, and $\mathbf{r}_T$ and $\mathbf{r}_P$ are the T-e and P-e relative coordinates, respectively.

Following a similar algebra as in Ref. 1, we find that in the symmetric-eikonal approximation[12] the electron-bremsstrahlung matrix element is given by

$$\langle H_l^{\mathrm{EB}}\rangle_{fi} = -iA_0\delta(\mathbf{U}_i - \mathbf{U}_f - \mathbf{k})I(\mathbf{P}'_T)\hat{\lambda}_l\cdot\mathbf{J}(\mathbf{P}'_P)\ , \quad (2.2)$$

where $\mathbf{U}_{i,f}$ are the initial and final total momenta of the mechanical system,

$$I(\mathbf{P}'_T) = \int d\mathbf{r}_T \exp(i\mathbf{P}'_T\cdot\mathbf{r}_T)\phi_i^*(\mathbf{r}_T)\phi_i(\mathbf{r}_T)\ , \quad (2.3)$$

$$\mathbf{J}(\mathbf{P}'_P) = \int d\mathbf{r}_P \exp(-i\mathbf{P}'_P\cdot\mathbf{r}_P)[E^-(Z_P,\mathbf{v};\mathbf{r}_p)]^* \times\nabla_{\mathbf{r}_p}E^+(Z_p,\mathbf{v};\mathbf{r}_p)\ , \quad (2.4)$$

$$\mathbf{P}'_T = \mathbf{P} - (M_T/M_3)\mathbf{k},\quad \mathbf{P}'_P = \mathbf{P} + (M_P/M_3)\mathbf{k}\ . \quad (2.5)$$

$\mathbf{P} = \mathbf{K}_i - \mathbf{K}_f$ is the momentum-transfer vector and $E^{\pm}$ are the Coulomb phases [see Eq. (3.10) of Ref. 1 or Eq. (8) of Ref. 12]. $\mathbf{J}(\mathbf{P}'_P)$ represents the bremsstrahlung term, while $I(\mathbf{P}'_T)$ does the atomic form factor. In the continuum distorted-wave approximation the usual Coulomb hypergeometric function ${}_1F_1$ replaces $E^{\pm}$.[12] In that approach the corresponding wave functions are not off-shell orthogonal. We have used the symmetric eikonal because it gives a very good agreement with the experiments for nonradiative excitation.[12] Integrating over $\mathbf{U}_f$ and the energy-conservation δ function corresponding to the probability of transition, the fivefold differential cross section finally reads

$$\frac{d^5\sigma}{d\omega\, d\Omega_\omega d\Omega} = \frac{v_T^2\omega}{(2\pi)^4c^3}\sum_{l=1}^{2}|I(\mathbf{P}'_T)\hat{\lambda}_l\cdot\mathbf{J}(\mathbf{P}'_P)|^2\ , \quad (2.6)$$

where c is the speed of light, v_T is the reduced mass of the $(T+e)$-P system, and $d\Omega = \sin\theta\, d\theta d\varphi$ is the differential solid angle of the scattered projectile,

$$P_z = \hat{\mathbf{v}}\cdot\mathbf{P} = \omega[1-(M_P/M_3)\beta\cos\theta_\omega]/v\ ,$$
$$P_x = -K_i\sin\theta\cos\varphi\ , \quad (2.7)$$
$$P_y = -K_i\sin\theta\sin\varphi\ ,$$

with $\beta = v/c$.

III. RESULTS

Photon distributions were obtained after performing numerical two-dimensional integrals (2.6) over θ and φ, AB cross sections with retardation for the process

$$\mathrm{H}^+ + \mathrm{Al}(1s) \rightarrow \mathrm{H}^+ + \mathrm{Al}(1s) + \omega \quad (3.1)$$

are displayed in Figs. 1–4. We have used hydrogenlike wave functions with effective charge $Z_T = 12.7$. Suffixes r and d denote retardation and dipole approximation, respectively. As the photon energy tends to zero retardation effects obviously become negligible, and the dipole approximation holds.

Figures 1(a) and 1(b) show photon angular distributions for proton energies 0.5 and 1.5 MeV, respectively. Experimental results of Ozawa *et al.*[13] and Ishii and Morita[9] are also displayed. Photon energies are in the 2.85–3.00 and 5.18–5.67 keV range which are larger than $T_m = 1.09$ and 3.26 keV, respectively, then AB is the dominant process to the x-ray production. The dipole approximation exhibits the well-known symmetric shape, and retardation effects present a forward-shifted distribution reproducing the asymmetry of the experiments.

Figure 2(a) shows the spectrum at 90° to the beam at 2-MeV proton energy. It should be noted here that retardation effects are null when measurements are made perpendicular to the beam. As observed, AB becomes relevant from $\omega \gtrsim T_m = 4.3$ keV on. In Fig. 2(b), ratios to 90° are displayed as a function of the photon energy and

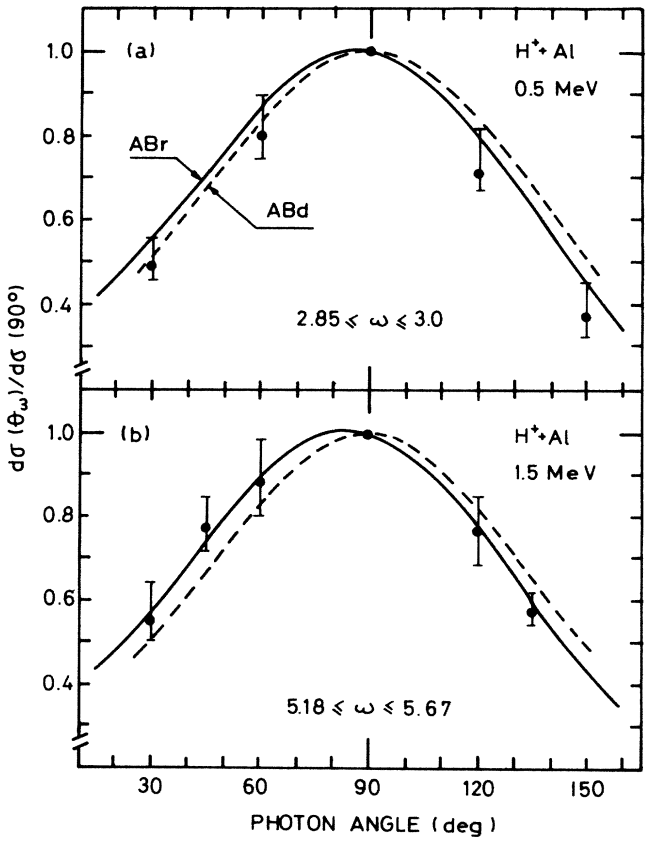

FIG. 1. (a) X-ray angular distributions for 0.5-MeV protons impinging on aluminum for photon energies in the range indicated. Theory: Throughout the figures we adopt the following notation: AB and SEB indicate atomic bremsstrahlung and secondary electron bremsstrahlung, respectively. The suffixes d and r denote dipole approximation and retardation, respectively. The experiments were performed by Ozawa *et al.* (Ref. 13). (b) Similar to (a) for 1.5-MeV proton energies. The experiments were performed by Ishii and Morita (Ref. 9).

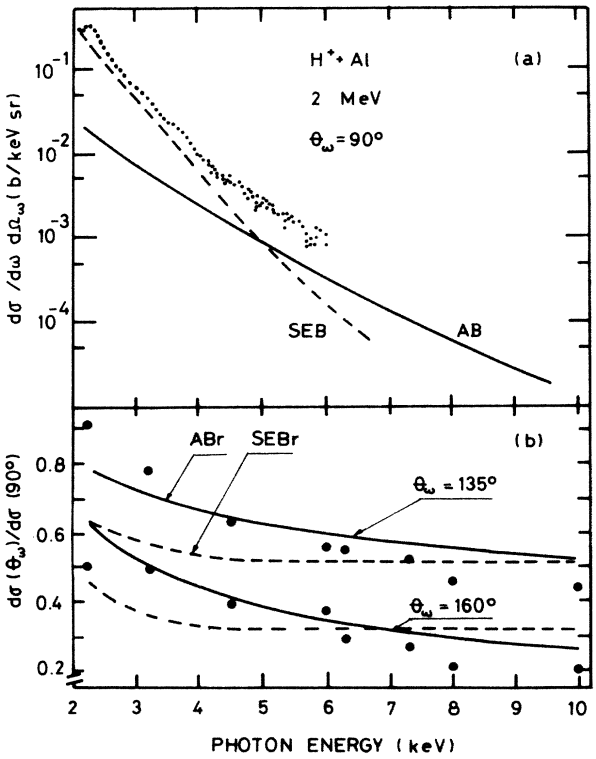

FIG. 2. (a) X-ray production at 90° to the beam for 2-MeV protons colliding with the aluminum target. Theory: Same as in Fig. 1(a). SEB as reported by Ishii *et al.* (Ref. 5) using the expression of Folkmann (Ref. 4). AB is our calculation (note that at 90° retardation effects are null). The experiments were performed by Ishii *et al.* using H_2^+ ions instead of protons. (b) Ratios of x-ray production cross section at 135° and 160° for the same system. The experiments were performed by Folkmann *et al.* (Ref. 14).

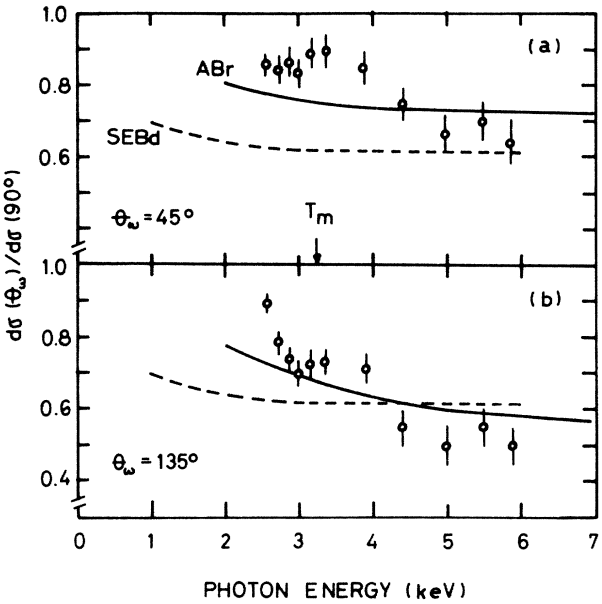

FIG. 3. (a) Ratios of x-ray production cross sections at 45° to those at 90° obtained with 1.5-MeV protons on aluminum. Theory; Same as in Fig. 1(a). The experiments were performed by Ishii *et al.* (Ref. 5). (b) Similar to (a) for 135°.

compared with SEB prediction, as reported by Folkmann *et al.*[14] Unexpectedly, for small ω (say $\omega < T_m$), where SEB should be the main mechanism for most of the x-rays production, the corresponding theory does not convincingly agree with the experiments. From T_m on, AB presents a reasonable agreement with the slope and values of the experiments. At very high photon energies, the internuclear bremsstrahlung should be taken into consideration.

Similar ratios are displayed in Figs. 3(a) and 3(b) and compared with the experiments of Ishii *et al.*[55] and theoretical predictions of SEBd as reported by the same authors. ABr seems to follow the data more closely except in the region between 3 and 4 keV where it does not reproduce the experimental enhancement.

For photon energies around T_m, SEB and AB are competitive and should be added as follows:

$$\frac{d\sigma(\theta_\omega)}{d\sigma(90°)} = p^{\mathrm{SEB}}(\omega)\frac{d\sigma^{\mathrm{SEB}}(\theta_\omega)}{d\sigma^{\mathrm{SEB}}(90°)} + p^{\mathrm{AB}}(\omega)\frac{d\sigma^{\mathrm{AB}}(\theta_\omega)}{d\sigma^{\mathrm{AB}}(90°)} , \tag{3.2}$$

where $p^X(\omega)$ are the corresponding weights given by

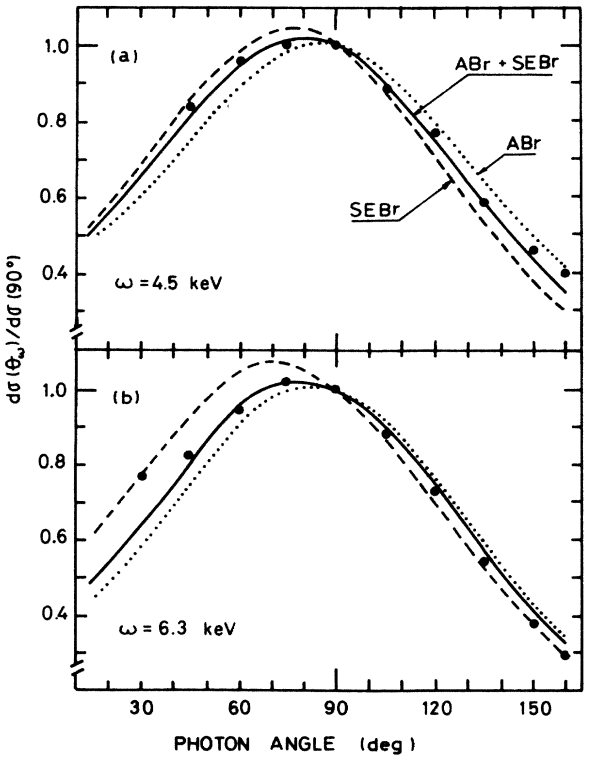

FIG. 4. (a) X-rays angular distributions for 2-MeV protons impinging on aluminum for a photon energy of 4.5 keV. Theory: Same as in Fig. 1(a). The solid line denotes the weighted sum as in Eq. (3.2). The experiments were performed by Folkmann *et al.* (Ref. 14). (b) Similar to (a) for a photon energy of 6.3 keV.

$$p^X(\omega)=\frac{d\sigma^X(90°)}{d\sigma^{SEB}(90°)+d\sigma^{AB}(90°)},\quad X=\text{SEB,AB}\ . \tag{3.3}$$

In Fig. 4 we studied the case considered by Folkmann *et al.* [from Fig. 2(a), and Fig. 3 of Ref. 14]:[14]

$$\begin{aligned} &p^{AB}(4.5\text{ keV})=0.42,\quad p^{SEB}(4.5\text{ keV})=0.58\ , \\ &p^{AB}(6.3\text{ keV})=0.71,\quad p^{SEB}(6.3\text{ keV})=0.29\ . \end{aligned} \tag{3.4}$$

The theoretical results, by using the mixture given by Eq. (3.2), seem to give the best agreement with the experiments.

In conclusion, AB with retardation presents forward-shifted asymmetric distributions in accordance with the data. When both AB and SEB are competitive, experimental angular distributions can be explained with the mixture. This work extends to higher photon energies the conclusions of Ishii *et al.*[3] that PIXE measurements should be made at angles as far backwards as possible.

[1] A. D. González, J. E. Miraglia, and C. R. Garibotti, Phys. Rev. A **34**, 2834 (1986).

[2] M. C. Pacher, A. D. González, and J. E. Miraglia, Phys. Rev. A **35**, 4108 (1987).

[3] K. Ishii, M. Kamiya, K. Sera, S. Morita, and H. Tawara, Phys. Rev. A **15**, 2126 (1977).

[4] F. Folkmann, C. Gaarde, T. Huus, and K. Kemp, Nucl. Instrum. Methods **119**, 117 (1974).

[5] K. Ishii, S. Morita, and H. Tawara, Phys. Rev. A **13**, 131 (1976).

[6] A. Yamadera, K. Ishii, K. Sera, M. Sebata, and S. Morita Phys. Rev. A **23**, 24 (1981).

[7] T. C. Chu, K. Ishii, A. Yamadera, M. Sebata, and S. Morita Phys. Rev. A **24**, 1720 (1981).

[8] M. Ya. Amusia, Comment At. Mol. Phys. **11**, 123 (1982).

[9] K. Ishii and S. Morita, Phys. Rev. A **30**, 2278 (1984).

[10] K. Ishii and S. Morita, Nucl. Instrum. Methods B **3**, 57 (1984).

[11] R. Shakeshaft and L. Spruch, Phys. Rev. Lett. **38**, 175 (1977). See also Sec. III A of Ref. 1.

[12] C. Reinhold and J. E. Miraglia, J. Phys. B **20**, 1069 (1987).

[13] K. Ozawa, J. H. Chang, Y. Yamamoto, S. Morita, and K. Ishii, Phys. Rev. A **33**, 3018 (1986).

[14] F. Folkmann, K. M. Cramon, and N. Hertel, Nucl. Instrum. Methods B **3**, 11 (1984).